Laser-rf double-resonance spectroscopy in a storage ring

M. Kristensen, J. S. Hangst, P. S. Jessen, J. S. Nielsen, O. Poulsen, and P. Shi
Institute of Physics and Astronomy, University of Aarhus, DK-8000 Århus C, Denmark
(Received 2 March 1992)

Laser-rf double-resonance spectroscopy of the hyperfine transition between $F''=0$ and $F'=1$ in the metastable $^3S_1$ state of $^6Li^+$ was performed in 100-keV beam in the storage ring ASTRID. High efficiency of optical pumping was demonstrated for complex pumping schemes. A broadband (dc–6 GHz) rf device was designed and used for rf spectroscopy in the storage ring. The possibility of obtaining coherent rf signals (Ramsey fringes) from successive interactions with the same field was investigated. Important limitations for the coherences due to magnetic-field inhomogeneities were observed. These led to randomization of the atomic polarization during only one turn in the storage ring and completely prevented observation of Ramsey fringes. This situation is different from the case of fundamental particles in a storage ring, where the polarization may be preserved for many round-trips. Limits were put on the demands to beam quality, beam positioning, and magnetic-field quality to overcome the problem. The effects of the rf device on the external degrees of freedom of the ion beam were investigated. Its small aperture substantially reduced the beam lifetime, and at very low rf frequencies the electric field in the rf device was able to excite external transverse resonances in the beam.

PACS number(s): 32.80.Bx, 29.20.Dh, 32.30.Bv

INTRODUCTION

Since the invention of techniques for rf spectroscopy in neutral beams in the 1930s [1], continued development has led to the creation of elegant spectroscopic methods [2]. In addition to the spectroscopic applications, a significant number of experiments has been aimed at the investigation of fundamental properties of nature [3,4] or toward the construction of extremely accurate clocks [5].

The most frequently used method for high-precision experiments is to pass a particle beam through two rf cavities and observe the coherent interactions between the particles and the rf [6]. For neutral particles the detection can conveniently be done by passing them through state-selecting inhomogeneous magnetic fields. For ions the most direct method is optical detection. Laser-rf double-resonance techniques have been refined for this purpose in fast beams [7]. A general problem encountered in working with ions in a beam is the space charge, which causes the beam to diverge within some μs, severely limiting the obtainable coherence time. This problem has been overcome in rf and penning ion traps, where infinite coherence times are in principle possible [3]. There are, however, some limitations to the method. If very precise measurements are needed, it is necessary to work with only one ion in the trap. Some types of ions such as metastable or radioactive species are not easy to produce and keep in traps. Finally, trap experiments are not made in field-free space.

Another possibility to control the space charge is to do the experiments in a storage ring. The idea of returning the particles to the same rf device several times and studying their coherent interactions with the rf was originally suggested by Ramsey in a different context [8]. It has several advantages compared to single-pass experiments. For instance, it is possible to do detection and optical pumping in collinear geometry without shifting the rf resonances due to the ac Stark effect, which is sometimes cumbersome in conventional collinear fast-beam laser-rf double-resonance spectroscopy [9]. The optical pumping is efficient, even in cases where the pumping transition is weak or when several photons of different frequencies might be needed. Finally, there exists no unknown phase shift between two rf devices as in the single-pass experiments.

In principle there are also some advantages compared to trap experiments. In traps laser cooling is needed in order to reduce the Doppler width significantly. In the storage ring longitudinally cold beams of any ion are readily available due to the velocity compression during acceleration. Using frequency filters, the Doppler shift for the fast stored beam enables suppression of noise from laser light scattered on the chamber walls. This possibility does not exist in traps.

The present experiments demonstrate several of these advantages for laser-rf double-resonance spectroscopy of metastable $^6Li^+$ in a 100-keV beam stored in the storage ring ASTRID. Experience also shows that some disadvantages exist for the technique. The main disadvantage is that the inhomogeneous magnetic fields, needed to confine the ions transversely, eliminate the coherence. Our measurements show no evidence of coherent interactions, even after only one round-trip in the storage ring. We put some limits on the demands to beam size and position control to improve this situation, and we show that these conditions might be within reach in the future, but will demand efficient transverse cooling.

A substantial reduction in the beam intensity and lifetime was observed when the rf device was inserted. This did not have any influence on the rf excitation, which takes place in a few turns, but it made the detection more difficult because of the reduced signal strength. The

transverse electric field in the rf device only had influence on the external degrees of freedom of the beam at frequencies below 100 MHz, far from the 3 GHz used for spectroscopy.

EXPERIMENTAL SETUP

Figure 1 shows a schematic diagram of the storage ring ASTRID. The ring has a circumference L_{ring} of 40 m and it is kept at a pressure of 3×10^{-11} Torr. The magnetic lattice, which confines the ions, consists of four pairs of bending magnets and 16 quadrupole magnets. For fine adjustments of the beam position the ring is equipped with 16 correction dipole magnets. The beam position can be measured with 16 electrostatic pickups. The ion beams are produced in a 200-keV accelerator, which supplies a high-density, low-divergence beam with a ripple below 1 V on a several-second time scale. The beam is chopped with an electrostatic chopper to match the ring circumference and is injected into the ring with a magnetic septum and an electrostatic kicker. Up to 10^9 singly charged ions can be stored this way when the rf device is not inserted.

Inside the ring two lasers are overlapped with the ion beam in two different straight sections. In one of these straight sections detection takes place through a window looking transversely at the beam. The emitted light is collected by a telescope and detected by a photomultiplier (PMT). A narrow interference filter with a full width at half maximum of 0.6 nm discriminates against stray light from the laser, which is Doppler shifted 3.0 nm relative to the laser-induced fluorescence for 100-keV $^6Li^+$ ions. The velocity of the ions can be changed in front of the detector using a postacceleration tube. This significantly increases the freedom to excite different lines with the same laser.

The rf device is situated in the same straight section of the ring. It is a traveling-wave device, which consists of an inner rectangular conductor and an outer conductor of a rather complex shape, as shown in Fig. 2. The design is a further development of a more simple construction by Sen, Goodman, and Childs [10]. This shape optimizes the strength and homogeneity of the field at the position of the beam and ensures perfect matching to 50 Ω from dc to 6 GHz. The length of the rf device L_{rf} is 304 mm, and it has 5×8 mm^2 apertures at each end. It is connected to standard subminiature amphenol (SMA) connectors through special UHV feedthroughs mounted transversely in each end. Our 50-Ω rf source, which consists of an Ailtech frequency synthesizer (dc–4 GHz) and a 20-W traveling-wave tube (TWT) amplifier, is connected to one end and a 50-Ω termination to the other. In this way only a traveling field in the TEM mode is able to interact with the beam. The magnetic field is linear polarized in the horizontal plane. The propagation direction can be chosen freely with the outside connections and the whole system can be translated in or out of the

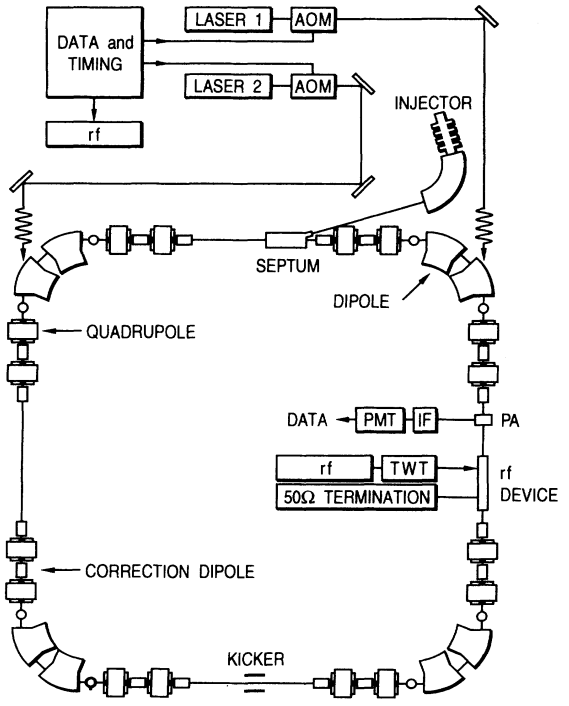

FIG. 1. Schematic diagram of the storage ring ASTRID, the 200-keV ion accelerator producing the ion beams and the laser and rf equipment used for the laser-rf double-resonance experiments. The timing and data acquisition system is also shown. The lasers can be modulated on or off with acousto-optic modulators and the rf can be modulated directly at the source.

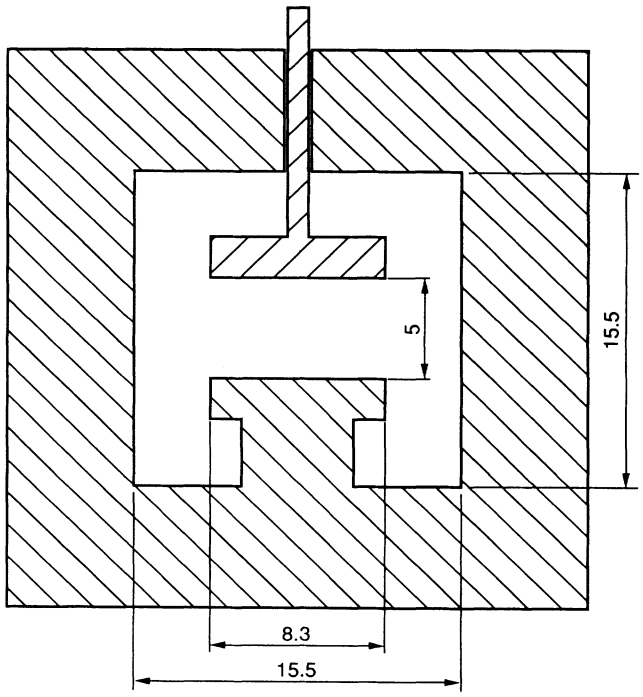

FIG. 2. Cross section of the rf device showing the inner rectangular conductor and the complicated cross section of the outer conductor. The inner conductor has a length of 304 mm and is mounted directly to SMA feedthroughs with a connection pin in each end.

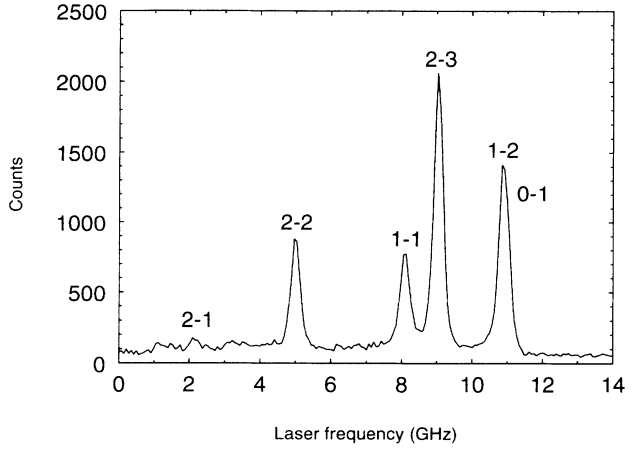

FIG. 3. 14-GHz scan of the $^3S_1 \rightarrow {}^3P_2$ transition in $^6Li^+$ with laser 1 performed on a dc beam to reduce the linewidth. The postacceleration was set at $U = 500$ V to reduce optical pumping.

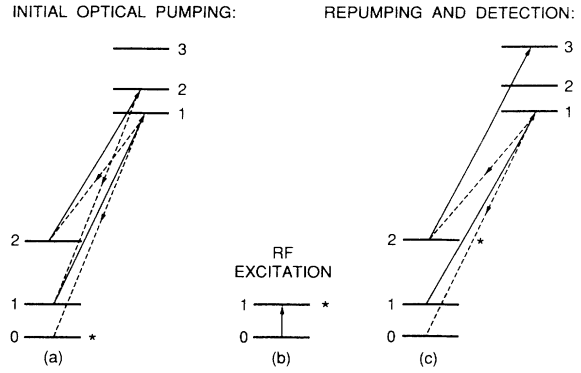

FIG. 4. Schematic illustration of the optical pumping, rf excitation, and detection. In part (a) the initial optical pumping using both lasers is shown together with the decay branching from the upper states. Part (b) shows the rf excitation. In part (c) the repumping and detection is described. For each step the most desired level, which the ions should ideally fall into, is marked with a star. For excitation back to $F = 2$ step (b) and step (c) are repeated several times.

beam. When the rf device is inserted into the beam, it is only possible to store approximately 3% of the original beam intensity (3×10^7 particles) for more than 100 μs.

The $^6Li^+$ ions are produced with a hot plasma ion source, which predominantly produces ground-state ions, but a small fraction of about 10^{-4} is present in the metastable $^3S_1$ state [11] and available for spectroscopy. The $^3S_1$ state is connected with the ^3P_n ($n = 0,1,2$) states (lifetime $\tau \approx 43$ ns) through allowed optical transitions around 548.6 nm in the rest frame. One of the lines ($^3S_1, F'' = 2 \rightarrow {}^3P_2, F' = 3$) is closed and therefore good for detection like the analogous line in $^7Li^+$ [12]. Several of the other lines to the $^3P_2$ levels can be used for optical pumping. A laser scan of the $^3S_1 \rightarrow {}^3P_2$ transition is shown in Fig. 3. The spectrum was taken with a dc ion beam of 15 μA, which passed once around the ring without the rf device inserted. The post acceleration was at 500 V to reduce effects from optical pumping in the rest of the straight section.

The width of the individual lines reflects an energy width at half maximum of ~ 20 V. This is much more than the energy spread from the accelerator. The fast heating after the acceleration is due to intrabeam scattering in the dense beam. It is in good agreement with theoretical expectations [13] and measurements for other ions in ASTRID [11].

OPTICAL PUMPING

The metastable part of the beam from the ion source had equal population of all nine (F, M_F) levels in the $^3S_1$ state. The purpose of the initial optical pumping is to accumulate the whole population in the $F = 0$ level. This was achieved by simultaneous excitation of the $F'' = 2 \rightarrow F' = 2$ and $F'' = 1 \rightarrow F' = 1$ lines as shown in Fig. 4, where the branching from the upper levels is also indicated. For every excitation there is a 50% chance of falling into the level most favorable for the transfer to $F = 0$. If both lasers are in resonance with a certain velocity class, the optical pumping will be completed within 10 to 20 lifetimes (less than 1 μs), independent of which level the ions are in initially. Due to the fast longitudinal heating of the beam after injection, most ions are not in perfect resonance with the laser. For the laser powers available during this experiment, it is possible to saturate the lines approximately 50 times, so the power-broadened linewidth was 25 MHz. This is less than 10% of the Doppler linewidth, even on the first turn. Therefore a substantially longer optical pumping time was needed. Furthermore each of the pumping lasers only had 8 m overlap with the ion beam in one straight section of the ring. All together these effects increase the necessary optical pumping time approximately two orders of magnitude. Experimentally, 110-μs optical pumping time was found to be an optimum compromise between efficiency and time.

It was possible to use the postacceleration tube to make a test of the optical pumping. The relationship between postacceleration voltage U, beam velocity v, and frequency shift $\Delta\nu$ of the counterpropagating laser, as it is seen from the ions' rest frame inside the post acceleration tube, is given by

$$\Delta\nu = -\left[\left[\frac{c}{v}\right]^2 - 1\right]^{1/2} \frac{\nu_0 e}{M_0 c^2} U = \left[-16.3 \frac{\text{MHz}}{\text{V}}\right] U \ . \tag{1}$$

Figure 5 shows a test of the optical pumping. Laser 2 was on from injection until 110 μs after injection in resonance with the $F'' = 2 \rightarrow F' = 2$ line. The postacceleration was set at -60 V, so laser 1 was cw in resonance with the $F'' = 1 \rightarrow F' = 1$ line outside the postacceleration and in resonance with the $F'' = 2 \rightarrow F' = 3$ line inside the postac-

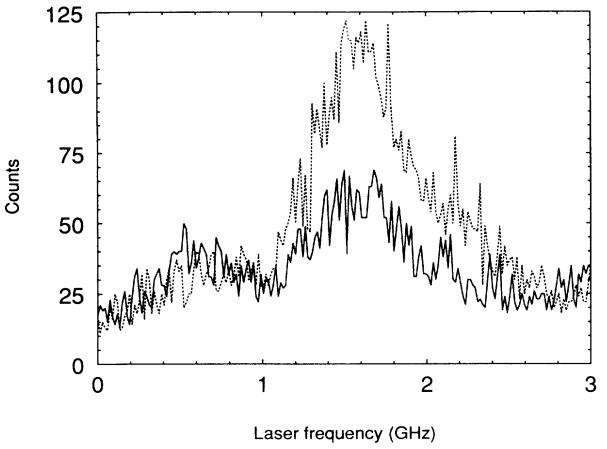

FIG. 5. 3-GHz laser scan near the $F''=2\rightarrow F'=3$ line to test the optical pumping. The dashed curve was recorded with laser 2 off. The solid curve was recorded with 2 on the first 110 μs after injection. The postacceleration was at $U=-60$ V to make laser 1 excite the $F''=1\rightarrow F'=1$ line outside the postacceleration, when it was in resonance with the $F''=2\rightarrow F'=3$ line inside the postacceleration. Detection was done during the first 2 ms after injection, and only one point was recorded for each injection.

celeration. The solid curve was recorded by stepping laser 1 in the vicinity of the $F''=2\rightarrow F'=3$ line (as seen from inside the postacceleration) one step per injection, and observing the fluorescence during the first 2 ms after injection. The dotted curve was recorded in the same way, but without laser 2. The lines in Fig. 5 are broader than the lines in Fig. 3 because they are recorded at a later time after injection, allowing intrabeam scattering to heat the beam further. The intensity of the $F''=2\rightarrow F'=3$ line is reduced roughly three times with laser 2 on, while the $F''=1\rightarrow F'=1$ line and the tail of the overlapping $F''=1\rightarrow F'=2$ and $F''=0\rightarrow F'=1$ lines are slightly more intense. This last effect occurs because laser 1, when detuned from the $F''=2\rightarrow F'=3$ line inside, is not in resonance with the $F''=1\rightarrow F'=1$ line outside the postacceleration. Therefore the ions pile up in the $F=1$ level when they are pumped away from the $F=2$ level by laser 2. Tests of the initial optical pumping where also made at later times after injection to confirm that the optically pumped ions stayed in the $F=0$ level.

Some ions are not pumped away from the $F=2$ level by the 110-μs optical pumping with laser 2. This is due to two effects. As mentioned above, 110 μs is not enough to totally complete the optical pumping. Second, there seems to be a continuous "increase" in the fraction of metastable $^6Li^+$ ions seen by the laser, probably due to an imperfect overlap between the laser and the ion beam immediately after injection [14]. The "new" metastable ions are populating all nine (F,M_F) levels equally, so in the optical pumping test and the rf experiment they appear as background. Other sources of background are laser light scattered on the walls on the vacuum chamber and dark counts from the PMT. Background doubled by photons scattered on the small aperture when the rf device was inserted.

rf EXCITATION

With one rf frequency it was impossible to directly excite from the $F=0$ level to the $F=2$ level, where detection could be done. The microwaves were generated with a 1 MHz to 4 GHz Ailtech frequency synthesizer, which was only able to produce the transition frequency between $F=0$ and $F=1$ at 3 GHz. Therefore the excitation to the $F=1$ level was made with the rf and the second step to the $F=2$ level with a laser 1 at the $F''=1\rightarrow F'=1$ line, as shown in Fig. 4.

The rf from the frequency synthesizer was amplified in a 20-W TWT amplifier, as seen in Fig. 1. The available rf power to interact with the beam in the rf device was only 15 W due to losses in the cables connecting the TWT to the rf section. The transition probability P_1 per passage of the rf section on perfect resonance is given by [9]

$$P_1=\sin^2(\tfrac{1}{2}t\Omega_R)\ ,$$

$$\Omega_R^2=\left[\frac{\mu_B g_J B_{\rm rf}}{\hbar}\right]^2(2F''+1)(2F'+1)(2J+1)(J+1)J \times\begin{Bmatrix}F'' & 1 & F'\\ J & I & J\end{Bmatrix}^2\begin{bmatrix}F'' & 1 & F'\\ M_{F''} & q & -M_{F'}\end{bmatrix}^2, \tag{2}$$

t is the transit time through the rf section, Ω_R is the Rabi frequency, μ_B is the Bohr magneton, $g_J=2$ is the g factor for the J level, $B_{\rm rf}$ is the magnetic-field strength inside the rf device, $I=1$ is the nuclear spin, and $q=\Delta M_F=\pm 1$. This gives 10% transition probability per round-trip for the $F''=M_{F''}=0\rightarrow F=-M_{F'}=1$ transition. For excitation four round-trips were used. If the transition probabilities add up incoherently, this leads to a total rf transition probability $P_{\rm rf}=30\%$. In general n independent round-trips with the rf on give the excitation probability

$$P_{\rm rf}(n)=\sum_{i=0}^{[(n-1)/2]}\begin{bmatrix}n\\ 2i+1\end{bmatrix}P_1^{2i+1}(1-P_1)^{n-(2i+1)}\ . \tag{3}$$

(The brackets in the upper summation index denote integer value.) If the transition probabilities build up coherently, it leads to an excitation probability on perfect resonance:

$$P_{\rm rf}(n)=\sin^2(\tfrac{1}{2}nt\Omega_R)\ . \tag{4}$$

Ω_R is given by formula (2). For four round trips this gives 92% rf transition probability.

Figure 6 shows a 20-MHz rf scan around the $F''=0\rightarrow F'=1$ transition frequency in $^3S_1$ to measure the incoherent rf transition. The single-pass rf excitation probability for frequencies detuned $\Delta=2\pi(\nu_0-\nu_{\rm rf})$ from perfect resonance is

$$P_1(\Delta)=\frac{\Omega_R^2}{\Delta^2+\Omega_R^2}\sin^2[\tfrac{1}{2}t(\Delta^2+\Omega_R^2)^{1/2}]\ . \tag{5}$$

The resonance data were fitted with this theoretical line shape. The spectrum was recorded with the rf counter-

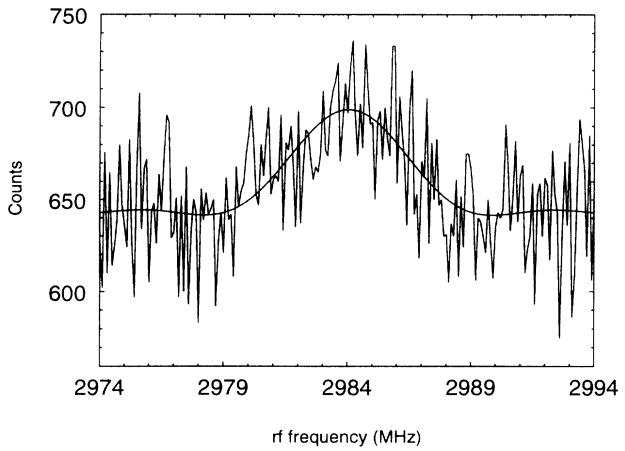

FIG. 6. 20-MHz rf scan of the $F''=0\rightarrow F'=1$ transition in the $^3S_1$ level. The rf was counterpropagating with the ion beam.

propagating with the ion beam. Similar spectra were also obtained with three and five round-trips, but no significant differences were observed between them. The connection between the rest-frame transition frequency ν_0, the frequency of the copropagating wave ν_+, and counterpropagating wave ν_- is given by the Doppler formula for both the rf and the lasers. The Doppler correction of the rf frequency to the rest-frame value was made using measurements of the optical transition frequency for the $F''=2\rightarrow F'=3$ line. The frequency of both lasers was measured using a phase-locked wave meter with a Zeeman-stabilized HeNe reference laser [15] calibrated against saturated absorptions in I_2 [16]. This setup was later tested against the Danish normal meter laser [17]. The rest-frame rf frequency is given by

$$\nu_0^{\mathrm{rf}}=\nu_-^{\mathrm{rf}}\left[\frac{\nu_+^{\mathrm{opt}}}{\nu_-^{\mathrm{opt}}}\right]^{1/2}, \tag{6}$$

where ν^{opt} is an optical frequency and ν^{rf} is an rf frequency.

In Table I the results from the incoherent rf measurements are collected together with the relevant optical frequencies for Doppler correction with formula (6). The beam energy $\bar{E}$ was calculated from the Doppler formula using the optical measurements

TABLE I. Results from the incoherent rf measurements together with the optical frequencies for the $F''=2\rightarrow F'=3$ line used for Doppler correction and the beam energy $\bar{E}$.

ν_+^{opt}	18 335.80(5) cm^{-1}	ν_-^m	2984.04(28) MHz
ν_-^{opt}	18 118.92(5) cm^{-1}	ν_0^m	3001.85(28) MHz
ν_0^{opt}	18 227.03(4) cm^{-1}	$\nu_0^{m\,a}$	3001.780(17) MHz
		t	0.170(1) μs
$\bar{E}$	99.14(10) keV	H_0	0.26(1) G
		$\Omega_R{}^b$	3.8(1) MHz
		$\Omega_R{}^c$	4.5(2) MHz
		S/N	9(1)%

[a]Reference [19].
[b]Formula (2).
[c]Fit value.

$$\bar{E}=M_0c^2\left\{\frac{1}{2}\left[\left[\frac{\nu_+}{\nu_-}\right]^{1/2}+\left[\frac{\nu_-}{\nu_+}\right]^{1/2}\right]-1\right\}. \tag{7}$$

The value for ν_0^{rf} is in good agreement with previous results obtained by Neumann [18]. The value for Ω_R was found from the fit in Fig. 6 keeping the value of the transit time t fixed. It deviates about three standard deviations from the value calculated from the field strength inside the rf section using formula 2. This indicates the presence of small distortions in the excitation line shape. These are discussed together with the detection.

RAMSEY FRINGES

After the investigation of the incoherent signal, a search for possible coherent excitations was conducted. If part of the rf excitation is coherent, it will show up as a regular modulation of the excitation probability. It is possible to calculate the excitation probability for all frequencies using the same method as for a classical Ramsey experiment [6]. This method consists of a direct integration of the time-dependent Schrödinger equation for an atom interacting with several oscillatory fields, without using the rotating-wave approximation. The Hamiltonian used in the simulation is given by

$$H=\begin{cases}H_a & \text{outside rf device}\\ H_0+\boldsymbol{\mu}\cdot\mathbf{B} & \text{inside rf device}\end{cases}. \tag{8}$$

H_a is the Hamiltonian describing the dynamics in the average field of the ring lattice and $\boldsymbol{\mu}\cdot\mathbf{B}$ is the perturbation from the microwave field, which is only present inside the rf device, where H_a is also replaced by the zero-field Hamiltonian H_0. A computer program was made that implements the method for a fast beam in a storage ring interacting n times with an rf field. There are a few differences between this situation and the classical situation in a slow atomic beam.

(i) The excitation takes place in a collinear geometry in a traveling-wave device instead of in a cavity.

(ii) Doppler shifts have to be described with the relativistic formula.

(iii) The time it takes the ion to move one round-trip between two interactions with the rf is given by $t_0=L_{\mathrm{ring}}/v$ at $\bar{E}$. If the beam energy is changed $\Delta\bar{E}$ from this value, the change in round-trip time is given by $\Delta t_0=\frac{1}{2}\eta t_0\Delta\bar{E}/\bar{E}$, where η is a parameter for the storage ring taking into account the change in orbit length that occurs simultaneously with the change in velocity. In a single-pass experiment η is always equal to 1, but for ASTRID it is equal to 0.947. This number was obtained by simulating the ring lattice of ASTRID with the MAD program (a standard CERN program for simulations in storage rings) [19].

(iv) The strength of the magnetic field varies substantially during one round-trip. This leads to a large and important difference between the zero-field energy difference ΔE_0 and the average energy splitting ΔE_a primarily due to the effect from the dipole magnets. The smaller contribution from the quadrupole magnets was neglected in

this simulation. The effects of it are described later. In this approximation the different beam trajectories do not have any influence on H_a and their influence is only taken into account through the difference in round-trip time and Doppler effect.

These four differences between a single-pass Ramsey experiment and the storage-ring experiment do not change the general structure of the results. There are, however, a number of small but important differences that appear.

The excitation line shape consists of a series of resonance peaks with a convolution curve given by the single-pass excitation line shape from formula (5), multiplied by a constant factor k_c, which can be found from formulas (2) and (4):

$$k_c = \frac{\sin^2(\frac{1}{2}nt\Omega_R)}{\sin^2(\frac{1}{2}t\Omega_R)} . \tag{9}$$

The distance between the individual peaks is given by the average inverse round-trip time $1/t_0$. The width of the individual peaks is slightly less than $1/(nt_0)$ for zero energy spread in the beam. This is illustrated with a simulation, shown in Fig. 7, of a Ramsey fringe experiment with four turns rf excitation and a single-pass probability leading to 92% excitation probability at the center. ΔE_a was 2.92 GHz and ΔE_0 was 3 GHz, the beam energy was 100 keV and the rf counterpropagating with the ion beam. The Doppler broadening was calculated by assuming that the laser could only interact sufficiently with the ions within a 250-MHz window to repump and detect them.

If these Ramsey fringes were observed it would be possible to determine ΔE_a for a given setting of the ring by performing the experiment with slightly different beam energies (and the same setting) or by changing the round-trip time with a second postacceleration section. If ΔE_a is determined in this way for a number of different settings of the ring, ΔE_0 can be found by extrapolating to zero magnetic field.

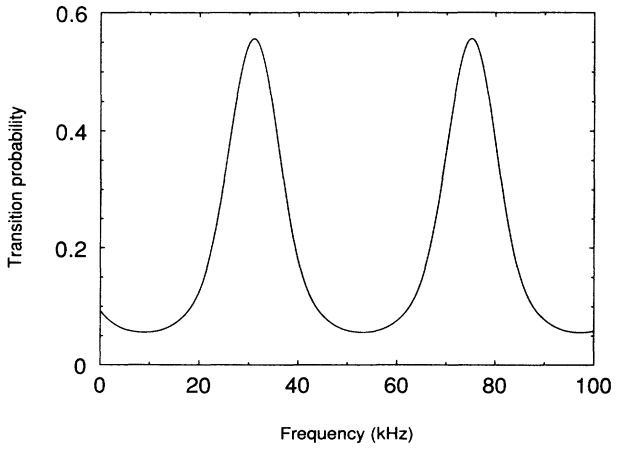

FIG. 7. Simulation of the coherent rf excitation line shape ignoring the influence from coherence-destroying inhomogeneous magnetic fields. The frequency window is centered around 2983.85 MHz.

The results from the simulation were used to set a limit for possible coherent contributions to the measured rf excitation. In reality ΔE_a may assume two different values for the two different final states $F=1$ and $M_F=\pm 1$. The value used in the simulation is close to the $M_F=-1$ result. Excitation to the level $F=1$, $M_F=0$ is not possible due to the polarization selection rule $\Delta M_F=\pm 1$ for excitation with a horizontally polarized B field. It is also not possible for the laser to repump from the $F=1$, $M_F=0$ level because $M_F''=M_F'=0$ is forbidden for $F''=F'$. As it is difficult to calculate the values of ΔE_a with the precision needed, and the saturation effects considered together with the detection further complicate the situation, a simple box function, instead of the spectrum in Fig. 7, was used during the analysis to set a maximum limit on coherent contributions.

Another difference between slow beam experiments in single-pass and storage-ring experiments is the possible cancellation of Doppler broadening and phase change broadening during one round-trip. A similar effect also exists in single-pass Ramsey experiments, where first-order broadening may be eliminated [2,6], but in the fast stored beam the effect is more complex because both the phase change and the Doppler effect are involved. A simple way of explaining a cancellation ultimately leading to first-order Doppler-free peaks is the following: If counterpropagating rf is interacting with an ion beam, ions with higher than average speed have a resonance frequency below the average due to the Doppler effect. The faster ions will simultaneously experience a shorter round-trip time than the average, and if $\nu_{\rm rf}$ is higher than $\Delta E_a/h$, this is the same as increasing the spacing between the local excitation maxima, which will move the peak towards higher frequencies. Depending on how well the η parameter, beam energy $\bar{E}$, ring circumference $L_{\rm ring}$, ΔE_a, and ΔE_0 match each other, variable degrees of cancellation might occur. If the sign of one of the parameters $(\nu_{\rm rf}-\Delta E_a/h)$ or the direction of the rf relative to the ion beam $(\pm)$ changes, the effect described above will increase the broadening instead of reducing it. A detailed look at the calculation leading to Fig. 7 shows that the broadening is reduced by approximately 25%. For $M_F=1$ there will instead by an increase of 25% because ΔE_a is then ~ 80 MHz higher than ΔE_0. This will partly smear out the fringes from the second transition. This is a further justification for using the box function to give the limit for coherent contributions.

Figure 8 shows a 100-kHz rf scan near the center of the incoherent transition. Its center frequency coincides with Fig. 7. If part of the rf excitation was coherent it would show up as a regular modulation of the excitation probability with a spacing of 45 kHz similar to the one in Fig. 7. No such modulation can be seen in the figure. To give a more precise limit the spectrum was filtered with the box function described before. In this way a maximum limit of $0.9\pm 0.6\%$ for coherent contributions was obtained. As this is not significantly different from zero, we conclude that no Ramsey fringes were observed. Fourier transformation or smoothing of the spectrum gives similar results. As an extra test the analysis was repeated for

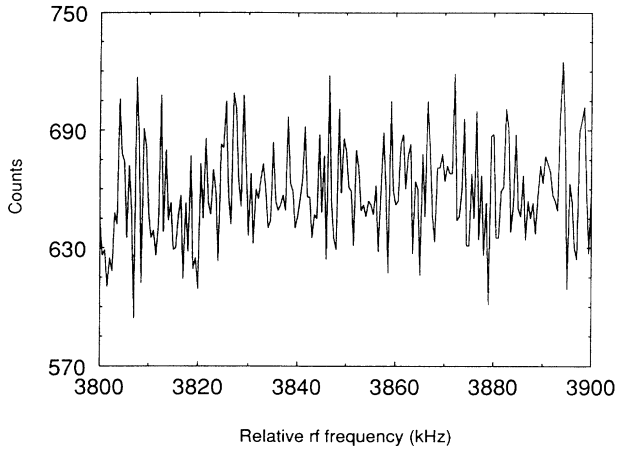

FIG. 8. 100-kHz rf scan near the center of the incoherent $F''=0\rightarrow F'=1$ transition to search for coherent contribution to the rf excitation.

a few other 100-kHz scans with different center frequencies. Similar results were obtained from these spectra.

DETECTION

After the rf excitation the repumping laser 1 was turned on for 90 μs. It was in resonance with the $F''=2\rightarrow F'=3$ line inside the postacceleration section and with the $F''=1\rightarrow F'=1$ line in the rest of the straight section. Including the necessary delays to avoid the laser and the rf being on simultaneously, the cycle took 189 μs. Only the $F''=1\rightarrow F'=1$ line could be used for this purpose, because the $F''=1\rightarrow F'=2$ and $F''=0\rightarrow F'=1$ lines were too closely overlapping. If the laser was put at one of these lines, it would automatically excite the other, and pump all the ions to the $F=2$ level independently of what the rf had done. The probability α_1 for pumping the ions into the $F=2$ level with laser 1 was only 4.8%, and the excitation with rf and pumping with the laser had to be done several times to get a reasonable signal. Because of the short storage lifetime of the beam when the rf device was inserted, the maximum number of repetitions was limited to about 50. Experimentally, it was found that the optimum was to repeat the cycle 20 times and do the detection between 1.89 and 3.89 ms. The detection could be started at any time, because the laser was in resonance with the $F''=2\rightarrow F'=3$ line inside the postacceleration section. Therefore it probed the number of ions in the $F=2$ level as shown in Fig. 4. Furthermore it is preferable to only be in resonance with the $F''=2\rightarrow F'=3$ line inside the postacceleration and everywhere else shifted to the red because off-resonant excitation of the $F''=0\rightarrow F'=1$ and $F''=1\rightarrow F'=2$ lines is reduced. This excitation and detection scheme was used both to measure incoherent rf transitions and to search for coherent transitions.

In Table I it can be seen that there are some minor deviations between the predicted and fitted line shapes for the incoherent rf excitation. To understand possible distortions of the rf excitation line shape it is necessary to consider saturation effects. These effects can occur for two reasons. One possible reason, during incoherent rf excitation, is that formula (3) is not linear in the single-pass rf excitation probability P_1. In the present experiments it gives rise to some broadening of the resonance, in agreement with the modified value for Ω_R. The expression for the single-pass rf excitation probability is symmetric around ν_0, so no shifts or asymmetries can occur due to saturation of the rf transition. Another type of saturation effect is due to the combined rf excitation and laser repumping. The probability of being excited from the $F=0$ level to the $F=2$ level $P_{F=2}$ after N repetitions of the rf and laser cycle is given by

$$P_{F=2}=1-(1-P_{\rm rf}\alpha_l)^N . \tag{10}$$

This expression is nonlinear in $P_n\alpha_l$ and can therefore also give rise to broadening. For incoherent rf excitation this effect will be small compared to the direct rf saturation. For pure coherent rf excitation the effect would be quite significant. The coherent rf excitation probability is almost symmetric around each excitation maximum, so only extremely small systematic shifts due to saturation can occur. These can always be ignored, because they will be of the order of $L_{\rm rf}/L_{\rm ring}$ ($<1\%$) times the width of the local excitation maximum.

The signal-to-noise ratio for the incoherent rf resonance is approximately 9%. This is in quite good agreement with the value expected from the test of the optical pumping and the numbers given above and leaves little room for coherent contributions to the excitation probability.

INFLUENCE FROM THE STORAGE RING

The most probable reasons for not observing coherent rf transitions are that the coherence for the whole population was destroyed by variations in the phase advance between different orbits through the ring, or that the ions did not stay in the same quantum state from one passage of the rf section until the next. The second effect can occur in two different ways. The ions can change F level or they can change M_F level. The tests of the optical pumping rule out the change of F level as an important effect in ASTRID. This is confirmed by theoretical calculations [20]. Left are the possibilities of changing M_F or having variable phase advance. Both effects can arise due to the inhomogeneous magnetic fields in the quadrupole magnets. The change in M_F level is most severe, because it also leads to a substantial difference in phase advance after passage of the next dipole magnet because of the M_F-dependent Zeeman effect.

Variable phase advance will occur when the magnetic field in a quadrupole has a component parallel to the dipole field for an ion passing through the quadrupole with a horizontal offset. If the quadrupole magnet is ideal, the field strength is proportional to the offset. This will introduce an extra phase change or modification of the energy ΔE_a, which will lead to a shift of the coherent resonance. If the ion beam has a finite size, this will lead to a broadening of the resonance. If we only consider one quadrupole and neglect the fringe field from it, we can

calculate the broadening $\Delta\nu_q$ as a function of the horizontal beam diameter D_h for a quadrupole of length L_q with quadrupole strength Q_s for the case of the linear Zeeman effect:

$$\Delta\nu_q = Q_s B_\rho D_h \Delta(g_F M_F)\mu_B \frac{L_q}{L_{\text{ring}}} \approx \left[30\frac{\text{MHz}}{\text{m}}\right] D_h \ . \quad (11)$$

B_ρ (0.11 T m for 100-keV $^6Li^+$) is the magnetic rigidity and $\Delta(g_F M_F)$ is the difference in g_F value multiplied with M_F for the two F levels involved. The 30 MHz/m is an approximate value for the $F''=0\rightarrow F'=1$ transition in a 100-keV $^6Li^+$ beam. The contribution from the next quadrupole magnet has a tendency to substantially reduce this number, because the quadrupoles are collected in pairs where one is focusing and the other defocusing with comparable strength in a particular plane. This cancellation is not totally perfect, partly because the betatron oscillations (due to the transverse beam temperature) around the central orbit will introduce asymmetries. From more careful considerations it is seen that a rough estimate of the effect after one round-trip in the ring can be found using the effect from only one (typical) quadrupole magnet [20]. The minimum requirement to observe coherent transitions is that the quadrupole broadening is smaller than the distance between the Ramsey fringes. From this we get an equation for the largest beam diameter $D_h^{\max}$ we can allow:

$$\Delta\nu_q(D_h^{\max})t_0 \leq 1 \ . \quad (12)$$

For our transition formula (12) gives $D_h^{\max}=1.5$ mm. To get an unperturbed result the diameter must be n times smaller than this number for excitation with rf on n round-trips.

The second case we will consider is the one with a magnetic field perpendicular to the dipole magnetic field. This will occur for ions that pass through a quadrupole magnet with a vertical offset. In this case the restriction on the beam diameter and offset from the center of the quadrupole magnets is that the precession of the magnetic moment μ must be much smaller than π during the passage of a quadrupole magnet. If it has to be smaller than 10% of π, formula (12) yields the maximum vertical beam diameter D_v, if D_h is exchanged by D_v:

$$\Delta\nu_q(D_v^{\max})t_0 \leq \tfrac{1}{10} \ . \quad (13)$$

Even a small precession of μ will mix the M_F levels substantially. This leads to a big difference in ΔE_a after passage of the next dipole magnet, which will totally exclude the survival of any coherence. Second, the partial back rotation of μ in the next quadrupole field can only be effective if the individual rotations in the two quadrupole magnets are small due to nonlinear effects.

For a real beam some combination of (12) and (13) will be relevant. A detailed quantum-mechanical analysis shows that these results obtained semiclassically also cover effects due to "Majorana" transitions, which take place in regions where the magnetic field is weak and changes direction rapidly [20]. The various restrictions for the beam diameters are collected in Table II. It should be noted once more that the numbers are only order-of-magnitude estimates. The precise numbers are extremely difficult to calculate [20].

TABLE II. Beam diameters and transverse temperatures $T_\perp$ needed to observe coherent rf transitions.

$F''=0\rightarrow F'=1$ in	100 keV $^6Li^+$	10 MeV $^6Li^+$
$D_v^{\max}$	0.15 mm	0.15 mm
$D_h^{\max}$ [a]	1.5 mm	1.5 mm
$T_\perp^{\max}$ [b]	0.4 K	40 K
$T_\perp^{\text{obs}}$	1000 K[c] 300 K[d]	500 K[e]

[a]One turn.
[b]Equal to ten turns.
[c]Reference [11].
[d]With rf device.
[e]Best results [12].

In general the requirements on beam quality and magnetic-field quality are orders of magnitude more severe than for beams of fundamental particles in high-energy storage rings. The reason for this problem is the magnetic-moment to mass ratio, which is the relevant parameter for describing polarization loss in a beam [21]. For an atomic ion it is of the order of μ_B/M_N, where M_N is the nuclear mass. For a fundamental particle it is of the order of μ_N/M_N, where μ_N is the nuclear magneton. The latter is more than three orders or magnitude smaller. Therefore it is only necessary to consider the problem of polarization loss close to polarization resonances in the machine, where the ions return to the same field inhomogeneities in phase on each turn or after a few turns (integer magnetic tune or other kinds of higher-order magnetic resonances). In case of a resonance the polarization destruction will build up coherently in a few turns.

An optical method was also used to test if position-dependent changes in M_F, which destroy the atomic polarization, were important in the storage ring. The $F''=1\rightarrow F'=0$ line in the $^3S_1\rightarrow{}^3P_1$ transition is ideal for this purpose. If it is excited with linear polarized light in the vertical plane defined by the dipole magnets, the population in the $F=1$ level will be optically pumped to the $M_F=\pm1$ levels as illustrated in Fig. 9, because of the selection rule $\Delta M_F=0$ for excitation with linear polarized light and the selection rule $\Delta M_F=0,\pm1$ for spontaneous decay.

The $^3S_1$, $F''=1\rightarrow{}^3P_1$, $F'=0$ line was excited cw inside

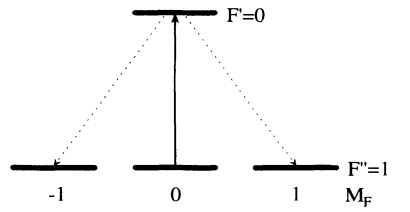

Fig. 9. Illustration of optical pumping among the M_F sublevels in the $F=1$ level, when the $^3S_1, F''=1\rightarrow{}^3P_1, F'=0$ line is excited with vertically polarized light. All ions are rapidly pumped to the $M_F=\pm1$ levels.

the postacceleration section with linear polarized light, and the fluorescence was detected the first 2 ms after injection. The current in a 50-turn solenoid located in the opposite straight section was then scanned between 0 and 20 A one step per injection. This allowed variation of the solenoid magnetic field is between 0 and $\sim 8\times 10^{-3}$ T. The optical signal during this scan of the magnetic field is shown in Fig. 10. If M_F was conserved with zero or any other finite current in the solenoid, there would be a modulation of the signal with the solenoid magnetic field. A minimum in fluorescence would occur for each N times 2π rotation of the magnetic moment in the solenoid field compared to the M_F conserving value. The period for this modulation would be 2 A. (Only the integral of the magnetic field is important for the number of rotations, when the magnetic field is weak. This integral is the same for all ions due to Ampere's circuital law.) No modulation of the signal was observed. Instead a small decrease was seen at the highest currents. This is due to a slightly skew mounting of some windings of the solenoid, which created an asymmetric fringe field disturbing the orbit in the ring. Tests at times later than 2 ms after injection gave the same result, but with poorer signal-to-noise ratio due to the heating of the beam and its finite lifetime. From this experiment it is concluded that the reason for not observing coherent rf transitions must be that all M_F levels mix within less than one turn.

In addition to these important effects from the storage-ring environment, it is necessary to consider a few other potential problems for coherent interactions.

The first question is whether ion-ion collisions can perturb the internal state of the individual ions. The risk of such a perturbation can be evaluated from a rough estimate of the cross section for state-changing collisions. A pessimistic estimate is to assume a geometrical cross section. If that were the case, there would be a probability for such a process of less than 10^{-7} per turn. This is comparable to the probability per round-trip for the same process due to collisions with the rest gas. It can be totally ignored compared to all other perturbations.

The second question is whether the direct influence of the electric field inside the rf device on the external degrees of freedom of the beam can be a problem. Below 100 MHz some influence on the beam was observed using the electrostatic pickups. At certain resonance frequencies it was possible to excite the beam transversely. This led to a beam lifetime of 10–100 turns. Above 100 MHz these resonances vanished abruptly and the rf had no measurable influence on the beam. It is assumed that the effect can be totally ignored at 3 GHz. This conclusion is supported by theory, because the oscillation of the electric field inside the rf device becomes so fast that its collective influence on the beam will average out to zero during a passage.

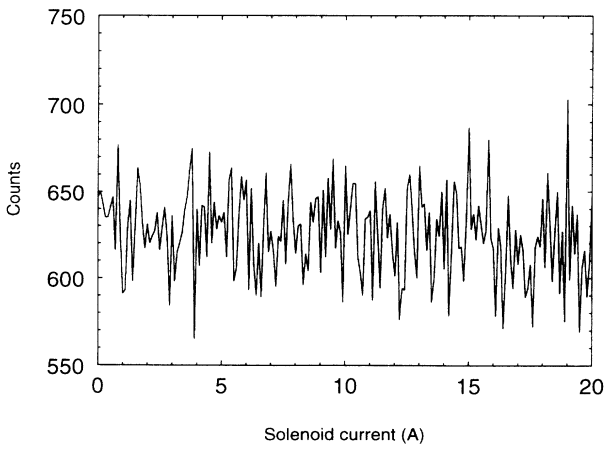

FIG. 10. 20-A scan of the current in the solenoid magnet. No modulation of the fluorescence was observed.

Finally, the influence from intrabeam diffusion due to Coulomb scattering on coherent interactions should be considered. The only way the diffusion can modify a coherent interaction is by changing the velocity and round-trip time of the ions. This change needs to exceed the range of the repumping laser (~ 250 MHz) within the excitation time to be a potential problem. If this occurs, several complications might arise. The first-order effect is that the signal decreases, because ions which move beyond the repumping range within the excitation time will be lost. If some of these ions return to the laser range and get repumped at a later time, it might give rise to a broadening or shift of the resonance. The loss in beam intensity when the rf device is inserted reduces the importance of intrabeam diffusion so the ions do not diffuse outside ~ 100 MHz within one repumping cycle. This is below the limit for complications to occur.

INFLUENCE FROM THE AHARONOV-BOHM EFFECT?

An interesting question is whether the classical Ramsey result with the phase advance difference between two states given by $\Delta\varphi_R = -t_0\Delta E_a/\hbar$ per turn in the ring also holds, when the influence from the Aharonov-Bohm effect is included. Only if this is true will it be correct to use the number ΔE_a for the splitting outside the rf device.

To include the Aharonov-Bohm effect correctly, it is necessary to consider two effects that have been ignored until now. The effects both arise from the fact that an ion with a magnetic moment $\boldsymbol{\mu}$ moving in the magnetic field from the dipole magnets feels both the classical Lorenz force $\mathbf{F}_L = q\mathbf{v}\times\mathbf{B}$ and the magnetic force $\mathbf{F}_m = \nabla(\boldsymbol{\mu}\cdot\mathbf{B})$. As the magnetic force is dependent on the internal state of the ion, it will give rise to a state-dependent acceleration in the fringe field of the dipole magnets. This means an ion will follow slightly different orbits in the dipole magnets, depending on in which state it is. This will introduce a geometrical phase difference $\Delta\varphi_g = \Phi_B e/\hbar$, where Φ_B is the magnetic flux through the area between the two different curves. A second effect comes from the difference in dynamic phase $\Delta\varphi_d$ between the different orbits. This effect is more difficult to calculate. It has been shown by Iida and Weidenmüller [22] that the two effects will in general cancel, and the classical Ramsey result is still valid. An excellent summary of the necessary arguments and calculations to obtain this result has been made by Forck [23].

CONCLUSION

Our laser-rf double-resonance experiments in the storage ring illustrate the possibility of using a complex optical pumping scheme and doing several successive incoherent rf excitations, which extend the applicability of fast-beam laser-rf double-resonance methods to some otherwise difficult cases.

The measured value for the frequency of the $F''=0\rightarrow F'=1$ transition in $^6Li^+$ is in good agreement with the value measured by Neumann and co-workers [18], but not quite as accurate because the relatively high beam energy gives a substantial transit-time broadening. If coherent transitions could be observed, this problem would be solved, but instead there would be some difficulty of extrapolating the result to zero magnetic field.

We do not observe coherent transitions because the magnetic fields inside the quadrupole magnets destroy the polarization of the beams. The theoretical calculations and the experiments are in good agreement on this point. Improvements in the measurements in the present type of storage ring can only be expected if the beam quality is increased substantially. From the theoretical estimates we find that the beam diameter must be below 0.15 mm. With the rf device inserted we have a beam diameter below 4 mm. A reduction of approximately 25 times is needed.

An improvement in the vertical beam positioning is also needed. In the present experiments we find that the vertical beam positions were correctly in the middle of the quadrupole magnets to within 0.5 mm. This must be improved to below 0.15 mm. The horizontal beam positions are not quite as critical, so the present accuracy is sufficient. The field quality in the magnets also seems to be adequate. These restrictions on beam quality and vertical position are beyond present-day technical possibilities. For the beam position an accuracy of 0.2 mm is the limit of our present system. It may be possible to improve this to 0.1 mm.

For the beam diameter the problem is more severe. Some sort of transverse cooling is needed. For a 100-keV beam, electron cooling cannot be expected to be efficient because of the extremely low electron energy needed to match the beam velocity. Transverse laser cooling is in principle a possibility but it is not possible to perform within the 10 ms available, even for a beam where all the ions are coolable. Finally the space charge will be a fundamental limitation to obtaining the small diameter if the beam is too intense. For instance 0.15 mm is equal to the zero-temperature radius for 10^7 particles. If the beam energy is increased, the polarization loss becomes less severe, because t_0 becomes smaller with $\bar{E}^{-1/2}$, but the vertical beam position restrictions are unchanged.

Finally it should be noted that most of the problems for the coherent interactions are due to the quadrupole magnets. If the transverse confinement of the beam was done with electrostatic quadrupoles instead, only the quadratic Stark effect would be present. For the small field strengths needed for our low-energy ion beams, this would only have negligible influence.

ACKNOWLEDGMENTS

We gratefully acknowledge stimulating discussions with the Heidelberg group at the storage-ring TSR, especially discussions with Professor D. Habs, who pointed out many important details. One of us (M.K.) thanks the Danish Natural Science Research Council and the Danish Science Academy for financial support.

[1] I. I. Rabi, J. R. Zacharias, S. Millman, and P. Kusch, Phys. Rev. **53**, 318 (1938).
[2] N. F. Ramsey, Phys. Today **33** (7), 25 (1980).
[3] J. J. Bollinger, D. J. Heinzen, W. M. Itano, S. L. Gilbert, and D. J. Wineland, Phys. Rev. Lett. **63**, 1031 (1989).
[4] N. F. Ramsey, Annu. Rev. Nucl. Part. Sci. **32**, 211 (1982).
[5] D. J. Wineland, Science **226**, 395 (1984).
[6] N. F. Ramsey, *Molecular Beams* (Oxford University Press, New York, 1956).
[7] U. Nielsen, O. Poulsen, P. Thorsen, and H. Crosswhite, Phys. Rev. Lett. **51**, 1749 (1983).
[8] N. F. Ramsey, Rev. Sci. Instrum. **28**, 57 (1957).
[9] G. Borghs, P. De Bisschop, J. Odeurs, R. E. Silverans, and M. Van Hove, Phys. Rev. A **31**, 1434 (1985).
[10] A. Sen, L. S. Goodman, and W. J. Childs, Rev. Sci. Instrum. **59**, 74 (1988).
[11] J. S. Hangst, M. Kristensen, J. S. Nielsen, O. Poulsen, J. P. Schiffer, and P. Shi, Phys. Rev. Lett. **67**, 1238 (1991).
[12] S. Schröder, R. Klein, N. Boos, M. Gerhard, R. Grieser, G. Huber, A. Karafillidis, M. Krieg, N. Schmidt, T. Kühl, R. Neumann, V. Balykin, M. Grieser, D. Habs, E. Jaeschke, D. Krämer, M. Kristensen, M. Music, W. Petrich, D. Schwalm, P. Sigray, M. Steck, B. Wanner, and A. Wolf, Phys. Rev. Lett. **64**, 2901 (1990); and (private communication).
[13] A. H. Sørensen, in CERN Report No. 87-10, edtied by S. Turner (CERN, Geneva, 1987), p. 135.
[14] J. S. Hangst, Ph.D. thesis, Fermilab Chicago, 1992.
[15] T. Baer, F. V. Kowalski, and J. L. Hall. Appl. Opt. **19**, 3173 (1980).
[16] L. Hlousek and W. M. Fairbank Jr., Opt. Lett. **8**, 322 (1983).
[17] J.-M. Chartier, H. Darnedde, M. Frennberg, J. Henningsen, U. Kärn, L. Pendrill, J ianpei Hu, J. Petersen, O. Poulsen, P. S. Ramanujam, F. Riehle, L. Robertsson, B. Stählberg and H. Wahlgreen, Metrologia (to be published).
[18] R. Neumann, J. Kowalski, F. Mayer, S. Noehte, R. Schwarzwald, H. Suhr, K. Winkler, and G. zu Putlitz, in *Proceeding of the Fifth International Conference on Laser Spectroscopy,* edited by A. R. W. Mckellar, T. Oka, and B. P. Stoicheff (Springer, Berlin, 1981), p. 134; J. Kowalski, R. Neumann, S. Noehte, K. Scheffzek, H. Suhr, and G. zu Putlitz, Hyperfine Interactions **15**, 159 (1983).
[19] S. P. Møller (private communication).
[20] M. Kristensen, Ph.D. thesis, University of Århus, 1992; M. Kristensen, J. S. Nielsen, P. Shi, O. Poulsen, and J. S. Hangst, in *Beam Dynamics and Laser Cooling of Stored Ions,* ICAP, München, 1992 (World Scientific, Singapore, in press).
[21] B. W. Montague, Phys. Rep. **113**, 1 (1984).
[22] S. Iida and H. A. Weidenmüller (private communication).
[23] P. Forck, Diplomarbeit, Max Planck Institut für Kernphysik, Heidelberg, 1991 (German).